nMulti-stage Supply Restoration of Active Distribution Networks with SOP Integration

Jie Jian[a], Peng Li[a], Hao Yu[a]*, Haoran Ji[a], Jie Ji[a], Guanyu Song[a],

Jinyue Yan[b], Jianzhong Wu[c] Chengshan Wang[a]

[a] Key Laboratory of Smart Grid of Ministry of Education, Tianjin University, Tianjin 300072, China

[b] School of Business, Society and Engineering, Mälardalen University, Västerås 72123, Sweden

[c] Institute of Energy, School of Engineering, Cardiff University, Cardiff CF24 3AA, UK

Abstract: Supply restoration from outages is essential for improving the reliability of active distribution networks (ADNs) after fault isolation. Soft open point (SOP) can adjust the power flow among feeders and provide voltage support for power outage areas. Considering the sequential coordination of switching operation and SOP control mode selection, a multi-stage supply restoration method with SOPs is proposed for ADNs. First, the sequential energization is formulated, in which the impact of SOP control mode on restoration sequence is analyzed. By providing voltage support, the coordination of SOPs will rapidly energize the outage area and improve the voltage profile. Then, a multi-stage restoration model with SOPs is proposed, in which reconfiguration of switches and control mode selection of SOPs are coordinated in sequence to maximize the load recovery level of ADNs. Through the switching action-time mapping, secure operation is ensured during the entire supply restoration process. Finally, the effectiveness of the proposed method is validated on a modified IEEE 33-node distribution system and practical distribution networks with four-terminal SOP. Results show that the proposed method can fully exploit the potential benefits of SOPs and effectively enhance the load recovery level of ADNs.

Key words: active distribution network (ADN); distributed generator (DG); soft open points (SOP); multi-stage supply restoration; sequential switching operation

* Corresponding author. Mobile: (+86)13752185093.
E-mail address: tjuyh@tju.edu.cn.

Nomenclature

Sets		$L_{i,t}$	Binary variables indicating operation status of load at node i at time period t
Ω_{n}, Ω_{n}^{*}	Sets of all nodes and nodes in the outage area	$Y_{i,s}^{\mathrm{load}}$	Binary variables indicating operation status of load breaker of node i at time period t
$\Omega_{\mathrm{n},k}$	Set of nodes in region k	$Y_{ij,s}^{\mathrm{tie},+}$ / $Y_{ij,s}^{\mathrm{tie},-}$ $Y_{ij,s}^{\mathrm{sec},+}$ / $Y_{ij,s}^{\mathrm{sec},-}$	Binary variables indicating the positive/negative changes of the switching action on line ij in stage s, respectively
Ω_{b}, Ω_{b}^{*}	Sets of all lines and lines in the outage area	$P_{i,t}$,$Q_{i.t}$	Total active/reactive power injection at node i at time period t (kW, kvar)
$\Omega_{\mathrm{b}}^{\mathrm{sw}}$, Ω_{k}^{sw}	Sets of all switch lines and switch lines in region k	$P_{ij,t}$,$Q_{ij,t}$	Active/reactive power flow of line ij at time period t (kW, kvar)
$\Omega_{\mathrm{tie}}^{\mathrm{sw}}$, $\Omega_{\mathrm{sec}}^{\mathrm{sw}}$	Sets of tie switches and sectional switches related to the outage area	$P_{i,t}^{\mathrm{SOP}}$,$Q_{i,t}^{\mathrm{SOP}}$	Active/reactive power output of SOP at node i at time period t (kW, kvar)
$\Omega_{m}^{\mathrm{SOP}}$	Set of nodes connected to SOP m	$P_{i.t}^{\mathrm{SOP,L}}$	Active power loss of SOP converter at node i at time period t (kW)
$\Omega_{\mathrm{tie}}^{\mathrm{ava}}$, $\Omega_{\mathrm{SOP}}^{\mathrm{ava}}$	Sets of tie switches and SOPs connecting normal area without outage	$P_{i.t}^{\mathrm{DG}}$,$Q_{i,t}^{\mathrm{DG}}$	Active/reactive power injection by DG at node i at time period t (kW, kvar)
$\Omega_{\mathrm{n,DG}}$,$\Omega_{\mathrm{n,DG}}^{*}$	Set of nodes connected by all DGs and DGs in the outage area	$P_{i,t}^{\mathrm{L}}$,$Q_{i,t}^{\mathrm{L}}$	Active/reactive power consumption at node i at time period t (kW, kvar)
Indices		$l_{ij,t}$	Square of current magnitude of branch ij at time period t
i, j, g	Indices of nodes	$v_{i,t}$	Square of voltage magnitude at node i at time period t
m	Indices of SOPs	***Parameters***	
s	Indices of supply restoration stages	N_{N}	Total number of nodes
k	Indices of regions in the outage area	N_{R}	Total number of regions in outage
t	Indices of time periods	N_{T}	Total number of time periods
Variables		N_{s}	Total number of restoration stages
$E_{k,s}$	Energized status of region k in stage s (1/0)	$P_{i,t}^{\mathrm{L,ref}}$, $Q_{i,t}^{\mathrm{L,ref}}$	Forecasted active/reactive power consumption at node i at time period t (kW, kvar)

$A_{i,k}$	Indicator of whether node i belongs to region k (1/0)	$P_{i,t}^{\mathrm{DG,ref}}$	Forecasted active power generated by DG at node i at time period t (kW)
$A_{ij,k}$	Indicator of whether line ij belongs to region k (1/0)	A_m^{SOP}	Loss coefficient of SOP m
$X_{i,s}$	Binary variables indicating energized status of node i in stage s	S_m^{SOP}	Capacity limit of SOP m
$X_{ij,s}$	Binary variables indicating energized status of line ij in stage s	r_{ij}, x_{ij}	Resistance/reactance of line ij
$Y_{ij,s}^{\mathrm{sec}}$,$Y_{ij,s}^{\mathrm{tie}}$	Binary variables indicating operation status of sectional switch and tie switch on line ij in stage s, respectively	$\overline{U}$, $\underline{U}$	Upper/lower limit of system voltage (kV, kV)
$\beta_{ij,s}$, $\beta_{ji,s}$	Continuous variables indicating the orientation of line ij in stage s	$\overline{I_{ij}}$	Upper current limit of line ij (A)
$\alpha_{ij,s}$	Binary variables indicating operation status of switch line ij in stage s	U_0	Voltage reference value
$Z_{i,s}^{\mathrm{SOP}}$	Binary variables indicating whether VSC of SOP at node i adopts $U_{ac}\theta$ control in stage s	pf_i^{DG}	Power factor of DG at node i
$\gamma_{ij,s}^{\mathrm{sw}}$, $\gamma_{i,s}^{\mathrm{SOP}}$	Binary variables indicating the energizing sequence of switch line ij and SOP connected to node i, respectively	λ_i	Important factor of load at node i
$K_{t,s}$	Binary variables indicating whether ADN at time period t is related to network configuration and SOP control mode in stage s	ω_1,ω_2,ω_3	Weight coefficients associated with each term in the objective function
T_s	The starting time of stage s (hour)	C_{sw}, C_{loss}	Basic price parameters of switching operation and power loss
$W_{m,t}$	Binary variables indicating energized status of SOP m at time period t	T_{ij}^{tie}, T_{ij}^{sec}	Average operation time of tie switch and sectional switch on line ij, respectively (hour)

1. Introduction

Supply restoration is essential for the improvement of self-healing competence of active distribution networks (ADNs). After fault isolation, it is necessary to conduct rapid load recovery and to serve customers with high-quality power [1]. Conventional supply restoration generally

depends on coordinated switching operation in ADNs [2]. The evolution of advanced power electronics facilitates the further improvement of load recovery level [3]. Soft open points (SOPs) refer to novel power electronic devices installed to displace traditional tie switches [4]. It can continuously adjust power flow with rapid response and flexible control modes. Under fault conditions, SOPs can provide voltage support rapidly and effectively enlarge the scope of supply restoration [5]. Thus, utilizing the potential benefits of SOP in supply restoration is of great significance.

Previous works have investigated service restoration methods considering the coordination of various controllable resources in ADNs. Ref. [6] proposed a DG-based islanding method to supply a group of nodes by at least one DG working in grid-forming mode. However, system operation requirements, such as secure operation constraints and the proper operation of loads, are disregarded. Ref. [7] further presented a network simplification method for the fast restoration with DG, which is a static approach valid during the entire restoration period. Ref. [8] proposed an interesting dynamic reconfiguration method with high DG penetration, which can effectively adapt to the randomness of DG outputs. Ref. [9] presented an analytical global restoration method to minimize the operation actions under the coordination of load shedding, voltage regulation devices and DGs. Ref. [10] further developed a decentralized multi-agent restoration method with DGs and conventional switches to maximize the load recovery level with minimized switching times. In addition, restoration strategies of SOPs under fault conditions have also been studied. The performance of SOP in load restoration has been verified. Ref. [11] analyzed the supply restoration principles of SOP and extended the applicability of traditional fault analysis techniques to distribution networks with SOPs. Ref. [12] investigated the optimal coordination of multiple SOPs to improve the self-healing ability of ADN. Ref. [13] proposed a coordinated restoration method applicable to multiple SOPs with network reconfiguration to improve load

restoration level. In [14], an effective supply restoration method was further developed for unbalanced ADNs based on multi-terminal SOP.

However, some challenges remain for the utilization of SOP in supply restoration, which are summarized as follows: 1) The multiple time scales of controllable resources for supply restoration should be taken into consideration. SOP can actively adjust the power flow and rapidly respond to system disturbances with flexible control modes. By contrast, conventional switches cannot act frequently and require deployment time. Thus, the coordination of multiple SOPs and switching actions needs to be investigated to achieve a maximum recovery level. 2) Static supply restoration results in previous works could only obtain the final status of SOP control mode and network configuration process. However, the operation sequence is undetermined during the restoration process [15]. A further consideration is required to formulate the sequential coordination of SOP control modes and switch operation to guarantee the secure restoration of ADNs [16]. Also, the sequence of restoration actions will directly influence the total amount of recovered loads [17]. 3) The supply restoration model mathematically belongs to mixed-integer nonlinear programming (MINLP) [18]. The restoration problem is time-dependent and cannot be easily divided into a series of individual problems by time periods [19]. The computation burden and complexity will expand exponentially with the increase of time periods [20].

The introduction of multi-stage concept can describe the coordinated restoration and alleviate the computation burden by reducing the number of integer variables. Researches have been investigated on the multi-stage-based sequential restoration with a moderate computation burden. Ref. [21] developed a variable time-step MILP model to coordinate the switching operation and dispatchable DGs. The routing repair crews are further coordinated in sequence in the synthetic restoration method presented in Ref. [22]. Ref. [23] proposed an efficient MILP model to

coordinate the repair routes and dispatch time of various resources and developed an accelerating algorithm for the solving process. Ref. [24] proposed an interesting multi-stage restorative management method which can guarantee the operation constraints are not violated by the conduction of multiple restoration methods. It is promising to reduce the computation burden by formulating the restoration model based on multiple stages. The other usage of the multi-stage concept is to divide the restoration periods into stages based on the coordination of reconfiguration and other devices. Ref. [25] formulated the sequential switching actions and DG operation in a reconfiguration stage in detail and established a mixed-integer second-order cone programming (MISOCP) model for efficient solving. The multi-stage concept can be effective for the SOP-based supply restoration method coordinated with reconfiguration. However, the impact of SOP on operation sequence as well as SOP-based coordinated restoration needs further investigation.

Considering the sequential coordination of SOP and switching operation, this paper proposes a multi-stage supply restoration approach for ADNs with SOP. The main contributions are summarized as follows.

1) The impact of SOP control mode on the supply restoration sequence is analyzed. SOPs will rapidly energize the outage area with an improved voltage level by providing voltage support. The flexible restoration strategy of SOPs is further considered to coordinate the control mode selection of SOPs with the relatively slow operation of conventional switches.

2) The multi-stage supply restoration model with SOPs is established, in which time-series fluctuation of DGs is considered. A limited number of reconfiguration stages is coordinated with SOP operation. The multiple time-scale sequential coordination of SOPs and conventional switches is realized through the switch action-time mapping. The recovery level of critical loads is enhanced and the secure operation is ensured during the entire restoration process.

The remainder of this paper is organized as follows. Section 2 describes the problem formulation with sequential energization, in which the impact of SOP control mode on the supply restoration sequence is also analyzed. Section 3 proposes the multi-stage supply restoration method with SOPs, in which the reconfiguration of switches and control mode selection of SOPs are coordinated to improve the recovery level in multiple stages. The solution methodology is elaborated in Section 4. Section 5 provides the case studies on the modified IEEE 33-node distribution system and a practical distribution network with four-terminal SOP in Tianjin. Finally, conclusions are stated in Section 6.

2. Problem formulation with sequential energization

This section introduces the basic concepts of energizing status and sequential energization with SOPs. In multi-stage supply restoration, the action sequence of SOPs and switches directly determines energized status of outage areas and further influences load recovery level of ADNs.

2.1. Description of energized status

Energized status is used to represent the operation state of the outage area in each restoration stage. The determination of energized status is the basis of load restoration. Network partition based on sectional switches is conducted to further describe energized status of lines and nodes.

1) Energized status of regions

After fault isolation, the downstream feeder of the fault area will be de-energized. Considering that each feeder is equipped with sectional switches, a feeder can be partitioned into several regions [9]. Each region consists of a sectional switch, several non-switch lines and nodes, as shown in Fig. 1(a).

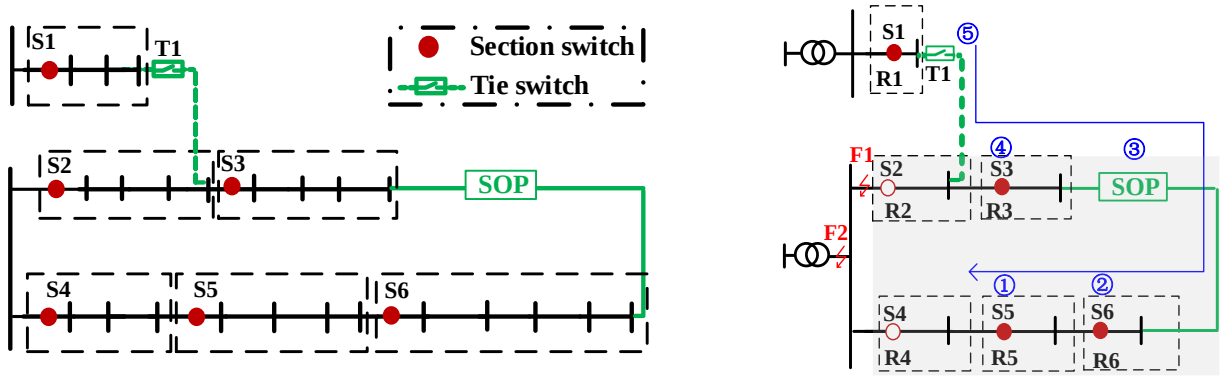

(a) Network partition **(b) Energizing path**

Fig. 1. Schematic of region partition in supply restoration

The energized status of a region is determined by the control mode of SOP and the operation status of switches connected to this region, as shown in (1).

$$E_{k,s} = \sum_{i\in\Omega_{\mathrm{n}}^{*}} A_{i,k}\left(\sum_{ij\in\Omega_{\mathrm{b}}^{\mathrm{sw}}} \beta_{ji,s} + \sum_{i\in\Omega_{m}^{\mathrm{SOP}}} Z_{i,s}^{\mathrm{SOP}}\right) \le 1 \tag{1}$$

where $\sum_{ij\in\Omega_{\mathrm{b}}^{\mathrm{sw}}} \beta_{ji,s}$ indicates the possible energizing paths from switches connected to region k. $\sum_{i\in\Omega_{m}^{\mathrm{SOP}}} Z_{i,s}^{\mathrm{SOP}}$ indicates the possible energizing paths from SOPs connected to region k.

Taking for example region R3 under fault F1 in Fig. 1(b), region R3 is energized if SOP or sectional switch S3 achieves connection of the region with the normal operation area.

2) Energized status of lines and nodes

The energized status of lines and nodes in the outage area is related to the energized status of regions. To be specific, the energized status of a node is consistent with the region status. As shown in (2.a), once a region is energized, all the nodes inside it are energized simultaneously.

$$X_{i,s} = \begin{cases} \sum_{k=1}^{N_{\mathrm{R}}}\left(A_{i,k}\cdot E_{k,s}\right), & i \in \Omega_{\mathrm{n}}^{*} \\ 1, & i \in \Omega_{\mathrm{n}}\backslash\Omega_{\mathrm{n}}^{*} \end{cases} \tag{2.a}$$

The energized status of lines is shown in (2.b). For a switch line, the energized status is decided by the switch connection status in each stage. For a non-switch line in the outage area, the energized status is the same as the related region status. For lines in the normal area without outage, lines remain energized.

$$X_{ij,s}=\begin{cases}\alpha_{ij,s} & , \ ij\in\Omega_{\mathrm{b}}^{\mathrm{sw}}\\ \sum_{k=1}^{N_{\mathrm{R}}}\left(A_{ij,k}\cdot E_{k,s}\right) & , \ ij\in\Omega_{\mathrm{b}}^{*}\backslash\Omega_{\mathrm{b}}^{\mathrm{sw}}\\ 1 & , \ ij\in\Omega_{\mathrm{b}}\backslash\Omega_{\mathrm{b}}^{*}\end{cases} \tag{2.b}$$

Eqs. (2.c) and (2.d) imply the operation status of sectional switches and tie switches, represented by the relevant energized status. When a sectional switch is opened ($Y_{ij,s}^{\mathrm{sec}}=1$) in a given stage s, the switch line is de-energized ($X_{ij,s}=0$) to disconnect the two end nodes. It means at least one of the two end nodes are energized ($X_{i,s}=1$ or $X_{j,s}=1$) and the two end nodes have different energized sources. Based on (2.c), for the sectional switches in other scenarios, $Y_{ij,s}^{\mathrm{sec}}$ is not subject to (2.c) and can get any value from {0, 1}. However, since the switching action is minimized in the objective function (5.c), $Y_{ij,s}^{\mathrm{sec}}$ will remain the same value as that in stage $s-1$. When a tie switch is closed ($Y_{ij,s}^{\mathrm{tie}}=1$), the tie line is energized, as shown in Eq. (2.d).

$$\begin{cases}Y_{ij,s}^{\mathrm{sec}}\geq\left(1-X_{ij,s}\right)+X_{i,s}-1\\ Y_{ij,s}^{\mathrm{sec}}\geq\left(1-X_{ij,s}\right)+X_{j,s}-1\end{cases}, ij\in\Omega_{\mathrm{sec}}^{\mathrm{sw}} \tag{2.c}$$

$$Y_{ij,s}^{\mathrm{tie}}=X_{ij,s} \quad , ij\in\Omega_{\mathrm{tie}}^{\mathrm{sw}} \tag{2.d}$$

2.2. Sequential energization with SOPs

The impact of SOP integration on the supply restoration sequence is analyzed to ensure the secure operation of ADNs.

1) Network connectivity constraints

The multi-stage restoration should ensure the radial topology of ADNs. First, the network connectivity constraint based on switch lines is formulated in (3.a) - (3.d).

$$0\leq\beta_{ij,s}\leq 1, \quad ij\in\Omega_{\mathrm{b}}^{\mathrm{sw}}=\Omega_{\mathrm{tie}}^{\mathrm{sw}}\cup\Omega_{\mathrm{sec}}^{\mathrm{sw}} \tag{3.a}$$

$$\beta_{ij,s}=\alpha_{ij,s}\,,\beta_{ji,s}=0, \ ij\in\Omega_{\mathrm{tie}}^{\mathrm{ava}} \tag{3.b}$$

$$\beta_{ij,s}+\beta_{ji,s}=\alpha_{ij,s}, \quad ij\in\Omega_{\mathrm{b}}^{\mathrm{sw}} \tag{3.c}$$

$$\alpha_{ij,s}\in\{0,1\}, ij\in\Omega_{\mathrm{b}}^{\mathrm{sw}} \tag{3.d}$$

where $\beta_{ij,s}$ and $\beta_{ji,s}$ are continuous variables to indicate the energizing direction of the switch line ij. If $\beta_{ij,s} = 1$, the energizing direction of switch line ij is from node i to node j. As for the tie switch connecting the outage area with the normal area without outage (R1 in Fig. 1(b)), the energizing direction is restricted by (3.b). Note that $\beta_{ij,s}$ and $\beta_{ji,s}$ are set as continuous variables to alleviate the computation burden by reducing the number of integer variables. Constraint (3.c) is further added to ensure the continuous variables $\beta_{ij,s}$ and $\beta_{ji,s}$ as 0 or 1 by restricting $\alpha_{ij,s}$ as integer variables.

The conventional switches can only connect the outage area with normal operating area as the energized source. Compared with conventional switches, SOP can adopt $U_{ac}\theta$ control and provide voltage support as the energizing source to the connected outage side. To ensure the radial topology, network connectivity constraints are modified with (3.e), considering the impact of SOP control mode.

$$\sum_{ji\in\Omega_b^{sw}} \beta_{ji,s} \le 1 - Z_{i,s}^{SOP} \tag{3.e}$$

where $Z_{i,s}^{SOP} = 1$ denotes that SOP provides voltage support to node i, resulting in $\sum_{ji\in\Omega_b^{sw}} \beta_{ji,s} = 0$. This means that node i connected to SOP is the parent node of adjacent nodes in stage s. For other nodes in the outage area, $\sum_{ij\in\Omega_b^{sw}} \beta_{ji,s} \le 1$ should be satisfied, which implies that each energized node has one and only one parent node.

2) Restoration energizing sequence with SOPs

The impact of SOP integration on the restoration sequence can be summarized into two aspects: First, SOP can rapidly respond to the system topology change and provide voltage support to de-energized regions. In addition, the energized SOP can provide power support to connected regions.

Considering SOP integration, the network connectivity constraint in (3) cannot guarantee the radial topology, as the possibility of isolated islanding areas energized by SOP and DG. The virtual flow approach in [20] is further modified to describe the restoration energizing sequence with SOP in (4). In each stage, virtual flow variables $\gamma_{i,s}^{\mathrm{SOP}}$ and $\gamma_{g,s}^{\mathrm{SOP}}$ are introduced for SOPs with $\gamma_{ij,s}^{\mathrm{sw}}$ and $\gamma_{ji,s}^{\mathrm{sw}}$ assigned to switch line ij.

$$\beta_{ij,s} \le \gamma_{ij,s}^{\mathrm{sw}} \le \mathrm{M} \cdot \beta_{ij,s}, ij \in \Omega_{\mathrm{b}}^{\mathrm{sw}} \tag{4.a}$$

$$Z_{i,s}^{\mathrm{SOP}} \le \gamma_{i,s}^{\mathrm{SOP}} \le \mathrm{M} \cdot Z_{i,s}^{\mathrm{SOP}}, i \in \Omega_{m}^{\mathrm{SOP}} \tag{4.b}$$

$$\sum_{i\in\Omega_{\mathrm{n},k}}(\gamma_{ji,s}^{\mathrm{sw}} + \gamma_{i,s}^{\mathrm{SOP}}) = \sum_{i\in\Omega_{\mathrm{n},k}}(\gamma_{ij,s}^{\mathrm{sw}} + \gamma_{g,s}^{\mathrm{SOP}}) + E_{k,s} \tag{4.c}$$

$$\sum_{ij\in\Omega_{\mathrm{tie}}^{\mathrm{ava}}} \gamma_{ij,s}^{\mathrm{sw}} + \sum_{ij\in\Omega_{\mathrm{SOP}}^{\mathrm{ava}}} \gamma_{i,s}^{\mathrm{SOP}} = \sum_{k=1}^{N_{\mathrm{R}}} E_{k,s}, \Omega^{\mathrm{ava}} = \Omega_{\mathrm{tie}}^{\mathrm{ava}} \cup \Omega_{\mathrm{SOP}}^{\mathrm{ava}} \tag{4.d}$$

As formulated in (4.a) and (4.b), at most one of virtual flow variables in pairs for a switch line or SOP can get a nonzero value, restricted by a large constant coefficient M. Then, a virtual flow balance equation is established based on its energized status of each region in (4.c). The energization of a region is assumed to consume the flow value of 1. The virtual flow value of a switch line or SOP is equal to the total number of the following energized regions on the energizing path. Eq. (4.d) implies the total virtual flow value provided by the tie switches and SOPs connecting the normal area with the outage area.

Taking for example the restoration under fault F2, R1 is the virtual energizing source of the entire outage area, connected by T1. Based on Eq. (4), an energizing sequence is indicated in Fig. 1(b). T1 has an energizing flow value of 5 to energize regions R2 to R6. The SOP has a value of 3 to energize regions R6 to R4. Switches S2 and S4 have a flow value of 0. Note that the energizing path is implied by the energizing flow value.

Thus, the radial topology is guaranteed with Eqs. (3) and (4), and restoration energizing sequence with SOPs and switches can be described by (4) considering the impact of SOP.

3. Multi-stage supply restoration method with SOPs

In this section, a multi-stage supply restoration model with SOPs is proposed, in which sequential switching operation is coordinated with SOPs to maximize the load recovery level.

3.1. Objective function

The proposed multi-stage supply restoration method with SOPs aims to achieve rapid supply restoration with an improved load recovery level. Besides, avoiding frequent switching actions and ensuring secure operation are also considered. Thus, a weighted linear combination of the minimum of active power of unrestored load (f_{R}) and operation costs of switching actions (f_{sw}) and power losses (f_{loss}) is taken as the objective function [28].

$$\min f = \omega_1 f_{\mathrm{R}} + \omega_2 (f_{\mathrm{sw}} + f_{\mathrm{loss}}) \tag{5.a}$$

$$f_{\mathrm{R}} = \sum_{t=1}^{N_{\mathrm{T}}} \sum_{i \in \Omega_{\mathrm{n}}} (1 - L_{i,t}) \lambda_i P_{i,t}^{\mathrm{L}} \tag{5.b}$$

$$f_{\mathrm{sw}} = C_{\mathrm{sw}} [\sum_{s}^{N_{\mathrm{s}}} \left(\sum_{ij \in \Omega_{\mathrm{tie}}^{\mathrm{sw}}} \left| Y_{ij,s}^{\mathrm{tie}} - Y_{ij,s-1}^{\mathrm{tie}} \right| + \sum_{ij \in \Omega_{\mathrm{sec}}^{\mathrm{sw}}} \left| Y_{ij,s}^{\mathrm{sec}} - Y_{ij,s-1}^{\mathrm{sec}} \right| \right) + \sum_{t=1}^{N_{\mathrm{T}}} \sum_{i \in \Omega_{\mathrm{n}}^{*}} Y_{i,t}^{\mathrm{load}}] \tag{5.c}$$

$$f_{\mathrm{loss}} = C_{\mathrm{loss}} \sum_{t=1}^{N_{\mathrm{T}}} (\sum_{ji \in \Omega_{\mathrm{b}}} R_{ji} l_{ji,t} + \sum_{i \in \Omega_m^{\mathrm{SOP}}} P_i^{\mathrm{SOP,L}}) \tag{5.d}$$

where ω_1 and ω_2 are the weight coefficients of the load restoration and operation economy objectives, respectively. The weight coefficients ω_1 and ω_2 are determined by DSO according to the consideration of their importance.

As focus of the restoration method, to minimize the active power of unrestored loads (f_{R}) has a much greater weight coefficient than the other objective ($\omega_1 \gg \omega_2$). Under fault conditions, f_{R} takes the major effect to regulate the operation of SOPs and switches to restore outage loads as ω_2 is a small positive value. Considering operational economy, the objective function of minimizing operation costs f_{sw} and f_{loss} will take effect after the critical loads are picked up.

3.2. Action-time mapping constraints

Considering the network topology will not change frequently, the restoration model is primarily built based on stages, which can reduce the number of binary variables [25].

The energized status of regions in each stage is described in (1) in Section 2.1. Energized status of nodes, lines and switches in each stage are described in (2) in Section 2.1. The radial topology constraints including energizing sequence with SOPs in a stage are established in (3) and (4) in Section 2.2.

Through action-time mapping, the above stage-related variables are correlated with the time-related power flow variables. The relationship between stages are also formulated using mapping variable $K_{t,s}$ in (6).

$$\begin{cases} \sum_{s=1}^{N_s} K_{t,s} = 1 & (6.a) \\ T_s - \mathrm{M}(1 - K_{t,s}) \le t \le T_{s+1} + \mathrm{M}(1 - K_{t,s}) & (6.b) \end{cases} \quad \forall t, s$$

$$T_s - T_{s-1} \ge \sum_{ij \in \Omega_{\mathrm{tie}}^{\mathrm{sw}}} \left| Y_{ij,s}^{\mathrm{tie}} - Y_{ij,s-1}^{\mathrm{tie}} \right| \cdot T_{ij}^{\mathrm{tie}} + \sum_{ij \in \Omega_{\mathrm{sec}}^{\mathrm{sw}}} \left| Y_{ij,s}^{\mathrm{sec}} - Y_{ij,s-1}^{\mathrm{sec}} \right| \cdot T_{ij}^{\mathrm{sec}} \quad (6.c)$$

In (6.a), $\sum_{s=1}^{N_s} K_{t,s} = 1$ denotes that each time period t is related to one and only one valid restoration stage s. Constraint (6.b) is used to correlate the time period $[T_s, T_{s+1}]$ to restoration stage s. If $T_s \le t \le T_{s+1}$, $K_{t,s} = 1$ should hold. If $t \ge T_{s+1}$ or $t \le T_s$, $K_{t,s} = 0$ should hold.

Constraint (6.c) is used to determine the duration of each stage. In a given stage, the switching action and SOP control mode are deployed in a successive manner. The response time of SOP is generally within milliseconds [4]. ADN undergoes the restoration stage $s-1$ from T_{s-1} to T_s. Thus, the duration of stage $s-1$ should be no less than the summed switching action time for stage s, as shown in (6.c). T_{ij}^{tie} and T_{ij}^{sec} are the average time to operate the related switches.

Based on (6), network configuration and control mode of SOP in each restoration stage are mapped to the corresponding time periods.

3.3. Restoration constraints of SOPs

Although SOP can respond quickly to the state change of system, load recovery level is limited by the capacity and location of SOPs [13]. The coordinated operation of multiple SOPs and conventional switches should be further considered.

1) Operation principles of SOPs

When the fault occurs in ADNs with SOP, SOP will be rapidly de-energized to reduce the influence of the fault area. After fault isolation, a re-energized SOP will rapidly take effect in supply restoration.

As SOP can transmit but not produce active power, the energized status of SOP depends on whether either VSC of SOP connects to an energized node in (7.a). SOP can provide power support once energized in (7.b). The operation constraints of SOP are formulated in (7.c) - (7.e).

$$\begin{cases} 0 \le W_{m-1,t} \le W_{m,t} \le 1 \\ W_{m,t} \le X_{i,s} + X_{j,s} + 1 - K_{t,s} \end{cases}, \quad i,j \in \Omega_m^{\mathrm{SOP}} \backslash \Omega_{\mathrm{SOP}}^{\mathrm{ava}}, \ \forall t,s \tag{7.a}$$

$$W_{m,t} = 1 \quad , \ m \in \Omega_{\mathrm{SOP}}^{\mathrm{ava}}$$

$$-\mathrm{M} \cdot W_{m,t} \le P_{i,t}^{\mathrm{SOP}} \le \mathrm{M} \cdot W_{m,t} \tag{7.b}$$

$$-\mathrm{M} \cdot W_{m,t} \le Q_{i,t}^{\mathrm{SOP}} \le \mathrm{M} \cdot W_{m,t}$$

$$P_{i,t}^{\mathrm{SOP}} + P_{j,t}^{\mathrm{SOP}} + P_{i,t}^{\mathrm{SOP,L}} + P_{j,t}^{\mathrm{SOP,L}} = 0 \tag{7.c}$$

$$\left(P_{i,t}^{\mathrm{SOP}}\right)^2 + \left(Q_{i,t}^{\mathrm{SOP}}\right)^2 \le (S_m^{\mathrm{SOP}})^2 \tag{7.d}$$

$$P_{i,t}^{\mathrm{SOP,L}} = A_m^{\mathrm{SOP}} \sqrt{\left(P_{i,t}^{\mathrm{SOP}}\right)^2 + \left(Q_{i,t}^{\mathrm{SOP}}\right)^2} \tag{7.e}$$

where $W_{m,t}$ denotes the energized status of SOP m at time period t. As shown in (7.a), SOP will be energized if any connecting node is energized at time period t in stage s ($X_{i,s} + X_{j,s} \ge 1, K_{t,s} = 1$). Constraints (7.d) and (7.e) are SOP capacity constraint and power loss equation [20], respectively.

2) Flexible coordinated strategies of SOPs

There are two aspects in the coordinated strategies of SOPs. One is the restoration strategy of an SOP under fault conditions. The other is the coordination of multiple SOPs and switches.

a) Control strategies of SOP include PQ-U_{dc}Q control and $U_{ac}\theta$-U_{dc}Q control under fault conditions. The related constraints are formulated in (7.f)-(7.h).

For each SOP in the outage area, at most one VSC provides voltage support and adopts $U_{ac}\theta$ control, as shown in (7.f). If SOP is energized from one side ($X_{j,s}=1$) and connected to an outage region on the other side, VSC on the other side will provide voltage support in (7.g) and (7.h).

$$0 \le Z_{i,s}^{\mathrm{SOP}} + Z_{j,s}^{\mathrm{SOP}} \le 1,\ 0 \le Z_{i,s}^{\mathrm{SOP}} \le 1 \qquad (7.f)$$

$$X_{j,s} \ge Z_{i,s}^{\mathrm{SOP}} \qquad i,j \in \Omega_m^{\mathrm{SOP}},\ \forall t,s \qquad (7.g)$$

$$v_{i,t} - U_0^2 \ge -\mathrm{M}\left[2 - W_{m,t} - Z_{i,s}^{\mathrm{SOP}}\right] \qquad (7.h)$$

b) Coordinated strategies among multiple SOPs and switching operation are described in (1) and (3.e). Considering multiple choices may be feasible for the same region, it is required that at most one of the possible sources can be chosen to energize this region. Besides, the energizing sequence of multiple SOPs can be revealed based on the virtual flow in (4).

3) Radial topology constraints

As shown in (3) and (4).

3.4. Power flow constraints of ADNs

Distflow branch model [29] is adopted to formulate the power flow constraints.

$$\begin{gathered}\sum_{ji\in\Omega_{\mathrm{b}}}\left(P_{ji,t} - r_{ji}l_{ji,t}\right) + P_{i,t} = \sum_{ig\in\Omega_{\mathrm{b}}} P_{ig,t} \\ \sum_{ji\in\Omega_{\mathrm{b}}}\left(Q_{ji,t} - x_{ji}l_{ji,t}\right) + Q_{i,t} = \sum_{ig\in\Omega_{\mathrm{b}}} Q_{ig,t}\end{gathered} \qquad (8.a)$$

$$\begin{gathered}P_{i,t} = P_{i,t}^{\mathrm{DG}} + P_{i,t}^{\mathrm{SOP}} - P_{i,t}^{\mathrm{L}} \\ Q_{i,t} = Q_{i,t}^{\mathrm{DG}} + Q_{i,t}^{\mathrm{SOP}} - Q_{i,t}^{\mathrm{L}}\end{gathered} \qquad (8.b)$$

$$v_{i,t} - v_{j,t} + \left(r_{ij}^2 + x_{ij}^2\right)l_{ij,t} - 2\left(R_{ij}P_{ij,t} + X_{ij}Q_{ij,t}\right) + \mathrm{M}\left(2 - X_{ij,s} - K_{t,s}\right) \ge 0, \qquad (8.c)$$

$$ij \in \Omega_{\mathrm{b}}, \forall t, s$$

$$v_{i,t} - v_{j,t} + \left(r_{ij}^2 + x_{ij}^2\right) l_{ij,t} - 2\left(R_{ij} P_{ij,t} + X_{ij} Q_{ij,t}\right) - \mathrm{M}\left(2 - X_{ij,s} - K_{t,s}\right) \le 0,$$

$$ij \in \Omega_{\mathrm{b}}, \forall t, s$$

$$\begin{aligned} -\mathrm{M}\left(X_{ij,s} + 1 - K_{t,s}\right) \le P_{ij,t} \le \mathrm{M}\left(X_{ij,s} + 1 - K_{t,s}\right), \\ -\mathrm{M}\left(X_{ij,s} + 1 - K_{t,s}\right) \le Q_{ij,t} \le \mathrm{M}\left(X_{ij,s} + 1 - K_{t,s}\right), \end{aligned} \tag{8.d}$$

$$0 \le l_{ij,t} \le (\bar{I}_{ij})^2 (X_{ij,s} + 1 - K_{t,s}) \tag{8.e}$$

$$(\underline{U})^2 (X_{i,s} + 1 - K_{t,s}) \le v_{i,t} \le (\bar{U})^2 (X_{i,s} + 1 - K_{t,s}) \tag{8.f}$$

$$l_{ij,t} v_{i,t} = P_{ij,t}^2 + Q_{ij,t}^2, ij \in \Omega_{\mathrm{n}} \tag{8.g}$$

In (8.c)-(8.f), the power flow variables at time period t are constrained by the network configuration and SOP control mode in stage s ($K_{t,s} = 1$). The switching operation and SOP control mode in irrelevant stages take no effect at time period t.

The power transmission and current of de-energized lines ($X_{ij,s} = 0$) are forced to be zeros in (8.d) and (8.e), respectively. In (8.f), the voltage magnitude of de-energized nodes ($X_{i,s} = 0$) is set to zero. Constraint (8.g) is the Ohm's law over line ij at time period t.

3.5. Pick-up constraints of loads and DGs

Assuming that each load is equipped with a breaker, loads may be shed initially to ensure secure operation. Load pick-up is scheduled in the subsequent restoration period.

$$\begin{cases} 0 \le L_{i,t-1} \le L_{i,t} \le 1 \\ L_{i,t} \le X_{i,s} + 1 - K_{t,s} \end{cases}, \quad i \in \Omega_{\mathrm{n}}^*, \forall t, s \tag{9.a}$$

$$Y_{i,t}^{\mathrm{load}} = X_{i,s} + 1 - K_{t,s} - L_{i,t}, \quad i \in \Omega_{\mathrm{n}}^* \tag{9.b}$$

$$P_{i,t}^{\mathrm{L}} = \begin{cases} L_{i,t} P_{i,t}^{\mathrm{L,ref}}, i \in \Omega_{\mathrm{n}}^*, \\ P_{i,t}^{\mathrm{L,ref}}, i \in \Omega_{\mathrm{n}} \backslash \Omega_{\mathrm{n}}^* \end{cases}, Q_{i,t}^{\mathrm{L}} = \begin{cases} L_{i,t} Q_{i,t}^{\mathrm{L,ref}}, i \in \Omega_{\mathrm{n}}^* \\ Q_{i,t}^{\mathrm{L,ref}}, i \in \Omega_{\mathrm{n}} \backslash \Omega_{\mathrm{n}}^* \end{cases} \tag{9.c}$$

As shown in (9.a), load pick-up is allowed at energized node i at time period t in stage s ($X_{i,s} = 1, K_{t,s} = 1$). Once the load at node i in the outage area is picked up ($L_{i,t} = 1$), no more shedding

is permitted in the following restoration period.

DG in the outage area is assumed to be energized and to inject power into the network once the connected node is energized ($X_{i,s}=1, K_{t,s}=1$), as formulated in (10).

$$\begin{aligned} & P_{i,t}^{\mathrm{DG}}-P_{i,t}^{\mathrm{DG,ref}}-\mathrm{M}\left(2-X_{i,s}-K_{t,s}\right)\le 0, \\ & P_{i,t}^{\mathrm{DG}}-P_{i,t}^{\mathrm{DG,ref}}+\mathrm{M}\left(2-X_{i,s}-K_{t,s}\right)\ge 0, \end{aligned} \qquad i\in\Omega_{\mathrm{n,DG}}^{*}$$

$$P_{i,t}^{\mathrm{DG}}=P_{i,t}^{\mathrm{DG,ref}} \qquad i\in\Omega_{\mathrm{n,DG}}\backslash\Omega_{\mathrm{n,DG}}^{*} \tag{10}$$

$$Q_{i,t}^{\mathrm{DG}}=P_{i,t}^{\mathrm{DG}}\cdot\sqrt{1-\left(pf_{i}^{\mathrm{DG}}\right)^{2}}/pf_{i}^{\mathrm{DG}} \qquad i\in\Omega_{\mathrm{n,DG}}$$

Considering the fluctuation of DG outputs [30], DG power support is utilized through the coordination of power transmission of SOP and switching operation in the multi-stage restoration.

The analytical formulation for the multi-stage restoration problem is provided in (11). The main decision variables consist of a) the line switching action in each restoration stage, b) the SOP control mode in each restoration stage, c) the power dispatch of SOPs at each time period, and d) the load switching action during the restoration period.

$$\begin{aligned} & \min f=\omega_{1}f_{\mathrm{R}}+\omega_{2}(f_{\mathrm{sw}}+f_{\mathrm{loss}}) \\ & \text{s.t. } (1)-(10) \end{aligned} \tag{11}$$

4. Solution methodology

The proposed restoration model in (11) is mathematically an MINLP problem due to the nonlinear objective (5.c) and constraints (6.c), (7.d), (7.e) and (8.g). As MISOCP has excellent performance of global optimality and calculation efficiency, it has been generally used to solve MINLP problems. The original model is transformed to the MISOCP model through convex relaxation for the feasibility and optimality of the solution [18].

Before convex relaxation, the nonlinear absolute term in (5.c) and (6.c) should be pre-processed to the linearized form. Auxiliary variables $Y_{ij,s}^{\mathrm{tie},+}$, $Y_{ij,s}^{\mathrm{tie},-}$, $Y_{ij,s}^{\mathrm{sec},+}$ and $Y_{ij,s}^{\mathrm{sec},-}$ are introduced to

reformulate (5.c) and (6.c) as (12.a) and (12.b), respectively. Constraints (12.c) and (12.d) are added as the equivalent constraints [31].

$$f_{\mathrm{sw}} = C_{\mathrm{sw}}[\sum_{s}^{N_{\mathrm{s}}}\left(\sum_{ij\in\Omega_{\mathrm{tie}}^{\mathrm{sw}}}\left(Y_{ij,s}^{\mathrm{tie},+}+Y_{ij,s}^{\mathrm{tie},-}\right)+\sum_{ij\in\Omega_{\mathrm{sec}}^{\mathrm{sw}}}\left(Y_{ij,s}^{\mathrm{sec},+}+Y_{ij,s}^{\mathrm{sec},-}\right)\right)+\sum_{t=1}^{N_{\mathrm{T}}}\sum_{i\in\Omega_{\mathrm{n}}^{*}}Y_{i,t}^{\mathrm{load}}] \tag{12.a}$$

$$T_s - T_{s-1} \geq \sum_{ij\in\Omega_{\mathrm{tie}}^{\mathrm{sw}}}\left(Y_{ij,s}^{\mathrm{tie},+}+Y_{ij,s}^{\mathrm{tie},-}\right)T_{ij}^{\mathrm{tie}} + \sum_{ij\in\Omega_{\mathrm{sec}}^{\mathrm{sw}}}\left(Y_{ij,s}^{\mathrm{sec},+}+Y_{ij,s}^{\mathrm{sec},-}\right)T_{ij}^{\mathrm{sec}} \tag{12.b}$$

$$\begin{gathered} Y_{ij,s}^{\mathrm{tie}} - Y_{ij,s-1}^{\mathrm{tie}} = Y_{ij,s}^{\mathrm{tie},+} - Y_{ij,s}^{\mathrm{tie},-} \\ Y_{ij,s}^{\mathrm{tie},+} + Y_{ij,s}^{\mathrm{tie},-} \leq 1,\ \ 0 \leq Y_{ij,s}^{\mathrm{tie},+}, Y_{ij,s}^{\mathrm{tie},-} \leq 1 \end{gathered} \tag{12.c}$$

$$\begin{gathered} Y_{ij,s}^{\mathrm{sec}} - Y_{ij,s-1}^{\mathrm{sec}} = Y_{ij,s}^{\mathrm{sec},+} - Y_{ij,s}^{\mathrm{sec},-} \\ Y_{ij,s}^{\mathrm{sec},+} + Y_{ij,s}^{\mathrm{sec},-} \leq 1,\ \ 0 \leq Y_{ij,s}^{\mathrm{sec},+}, Y_{ij,s}^{\mathrm{sec},-} \leq 1 \end{gathered} \tag{12.d}$$

Power flow constraints (8.g) over line ij at time period t can be relaxed to the second-order cone constraint (12.e) [32]:

$$\left\|\begin{bmatrix} 2P_{ij,t} & 2Q_{ij,t} & l_{ij,t} - v_{i,t} \end{bmatrix}^{\mathrm{T}}\right\|_2 \leq l_{ij,t} + v_{i,t}, ij \in \Omega_{\mathrm{n}} \tag{12.e}$$

The SOP operation constraints (7.d) and (7.e) are quadratic nonlinear constraints, which can be converted to the rotated quadratic cone forms [20] as follows:

$$\left(P_{i,t}^{\mathrm{SOP}}\right)^2 + \left(Q_{i,t}^{\mathrm{SOP}}\right)^2 \leq 2\frac{S_m^{\mathrm{SOP}}}{\sqrt{2}}\frac{S_m^{\mathrm{SOP}}}{\sqrt{2}} \tag{12.f}$$

$$\left(P_{i,t}^{\mathrm{SOP}}\right)^2 + \left(Q_{i,t}^{\mathrm{SOP}}\right)^2 \leq 2\frac{P_{i,t}^{\mathrm{SOP,L}}}{\sqrt{2}A_m^{\mathrm{SOP}}}\frac{P_{i,t}^{\mathrm{SOP,L}}}{\sqrt{2}A_m^{\mathrm{SOP}}} \tag{12.g}$$

Thus, the multi-stage restoration model can be reformulated as the following MISOCP model (13) after linearization and convex relaxation. The converted model (13) can be efficiently solved by a commercial solver, such as CPLEX or MOSEK [33].

$$\begin{gathered} \min f = \omega_1 f_{\mathrm{R}} + \omega_2 (f_{\mathrm{sw}} + f_{\mathrm{loss}}) \\ \text{s.t.}\,(1)-(4), (5.\mathrm{a}), (5.\mathrm{b}), (5.\mathrm{d})-(6.\mathrm{b}), (7)-(8.\mathrm{f}), (9)-(10), (12) \end{gathered} \tag{13}$$

The SOCP relaxation results in a small gap between the proposed model (13) and the original MINLP model (11). The relaxation deviation value is generally at the 1.0×10^{-5} level with tolerable accuracy [31]. To evaluate the accuracy of the conic relaxation, the infinite norm of relaxation deviation [34] is defined as follows.

$$\text{gap} = \left\| \frac{l_{ij,t} v_{i,t} - \left((P_{ij,t})^2 + (Q_{ij,t})^2 \right)}{l_{ij,t} v_{i,t}} \right\|_{\infty} \tag{14}$$

5. Case studies and analysis

The effectiveness of the proposed multi-stage restoration method with SOP is verified on a modified IEEE 33-node system and a practical distribution system with four-terminal SOP constructed in Tianjin.

5.1. Modified IEEE 33-node distribution system

The test case is based on a modified IEEE 33-node distribution system, as shown in Fig. 2. Sectional switches are labelled with red points and tie lines are labelled with green dotted lines. The rated voltage level is 12.66 kV. Total active power and reactive power demands are 3715.0 kW and 2300.0 kvar. The detailed parameters are shown in [35].

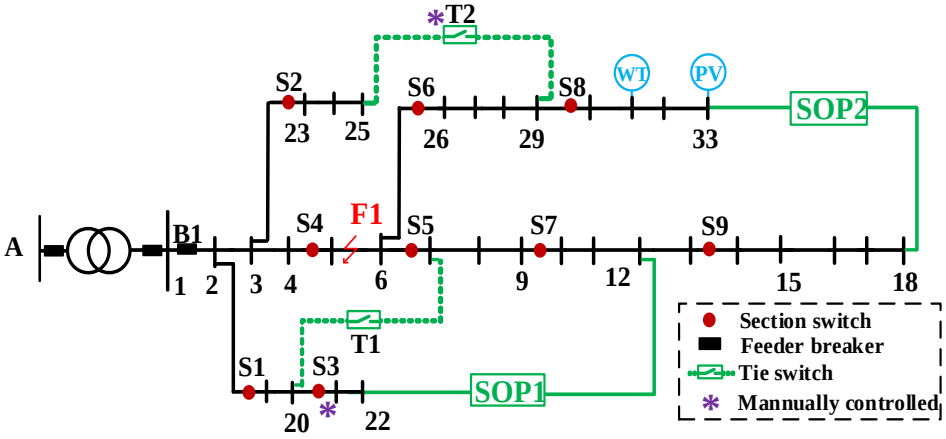

Fig. 2. Structure of the modified IEEE 33-node system.

To incorporate the impact of DG fluctuation, a PV unit with 400.0 kWp and a WT unit with 600.0 kVA are integrated into the network at nodes 31 and 33, respectively. The power factor of DG is assumed to be 1.0. The daily DG and load operation curves are given in Fig. 3 [32], taking 15 min as the unit time period. Two SOPs with the capacity of 800.0 kVA are installed between node 12 and node 22, as well as node 18 and node 33, to replace tie switches T3 and T4, respectively. Considering the high efficiency of power electronic-based inverters, the power loss coefficient of SOP is set to 0.01 [13].

The upper and lower limits of the secure voltage range are set to 1.05 p.u. and 0.95 p.u. As load recovery is the main priority in supply restoration, coefficients ω_1 and ω_2 are set to 100 and 0.7, which can be adjusted based on the requirements of operators. The cost coefficient associated with active power losses C_{loss}, that is, the unit price of electricity purchasing from the upper grid, is assumed as 0.076 USD/kWh in this paper. The cost coefficient related to variation of the switching operation C_{sw} is set as 1.547 USD/time, which can be adjusted according to the switching risk assessment of DSO [31].

To consider the supply priority of critical loads, the weight coefficients are adopted in Table 1. The manually controlled switch needs 30 min to be operated and is labeled with '*'. The operation time needed for a remotely controlled switch is 0.5 min. The maximum allowable number of switching actions of each switch is set to 3 throughout the entire restoration period.

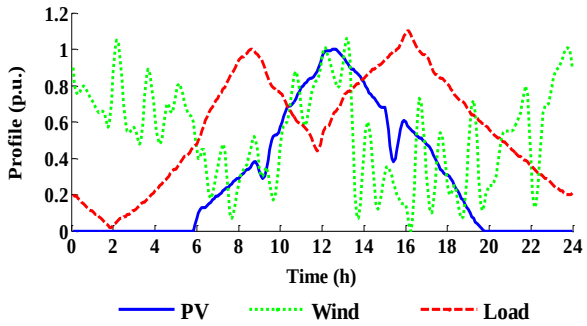

Fig. 3. Operation curves of DG and load.

Table 1 Weight coefficients of loads

Category	Weight coefficient	Node of load
I	100	8,24,32
II	1	1-7,9-23,25-31,33

The proposed model is performed in the YALMIP optimization toolbox [26] with MATLAB R2016a and solved by IBM ILOG CPLEX 12.6. The numerical experiments were executed on a computer with an Intel Xeon CPU E5-1620 processor running at 3.70 GHz and 32 GB of RAM.

5.2. Result analysis of multi-stage restoration

After fault isolation, the multi-stage coordination of SOPs and switches is conducted to maximize the load recovery level. Two schemes are used to verify the effectiveness of the proposed multi-stage restoration method with SOP.

Scheme I: Multi-stage supply restoration is conducted with only switches without SOPs.

Scheme II: Multi-stage supply restoration is conducted based on the coordination of SOPs and switches.

1) Multi-stage restoration with SOP integration

The line 5-6 is assumed has a permanent three-phase fault, which is defined as fault F1. The fault duration is assumed from 7:00 a.m. to 13:00 p.m. Under fault F1, switches S4, S5 and S6 are operated initially in Schemes I and II to isolate the fault. After fault isolation, nodes 7 to 18 and nodes 26 to 33 are de-energized and relevant loads and DGs are out of service. The total outage active power is 1995.0 kW. The above two schemes are conducted for supply restoration.

Supply restoration results are listed in Tables 2 and 3. The relaxation deviation value is at the 1.0×10^{-5} level with acceptable accuracy as shown in Table 3. Switching actions and SOP control modes in each stage are listed in Table 2 by the operation sequence. Supply restoration configuration in Schemes I and II are illustrated in Figs. 4 and 5. A node number in a blue dotted box

represents that the VSC of SOP connected to this node adopts $U_{ac}\theta$ control. Fig. 6 depicts the operation schedule of load breakers in Schemes I and II.

Table 2 Switching action and SOP control mode in fault scenario F1

Scheme	Stage	Switching action and SOP control mode
I	1 (7:00-7:30)	1) Open S7 and load breakers {18, 26, 30, 33}. 2) Close T4. 3) Close T1 and T3.
	2 (7:31-13:00)	1) Close T2 and open T4. 2) Close load breakers {30, 26, 33, 18} in sequence.
II	1 (7:00-7:30)	1) Open load breaker {31}. 2) SOP1 adopts $U_{ac}\theta$-$U_{dc}Q$ control. Then, SOP2 is energized and adopts $U_{ac}\theta$-$U_{dc}Q$ control. 3) Close T1. Then, SOP1 adopts PQ-$U_{dc}Q$ control and SOP2 remains $U_{ac}\theta$-$U_{dc}Q$ control.
	2 (7:31-13:00)	1) Close T2 and open S8. 2) Close load breaker {31}.

Compared with conventional tie switches, SOP shows an improved supply restoration capability due to flexible power flow control and voltage support. As shown in Table 3, Scheme II based on the multi-stage restoration with SOP has a better performance in load recovery level than Scheme I. Compared to Scheme I, the energy not supplied during the entire restoration period is decreased by 39.01% in Scheme II.

For Scheme I without SOP, supply restoration is conducted in two stages based on the network reconfiguration. The detailed load pick-up schedule in the supply restoration period is shown in Fig. 6(a). As listed in Table 3, load recovery level in Scheme I is limited by the voltage level.

Table 3 Supply restoration results of Schemes I and II

Scheme	Stage	Restored ratio of active power of loads (%)	Energy not supplied (kWh)	Voltage range (p.u.)	Operation cost (USD)	Gap (p.u.)

I	1	79.45	648.6250	0.9538-1.0000	51.95	1.087e-5
	2	100		0.9507-1.0000		
II	1	92.48	395.6250	0.9637-1.0498	36.00	1.625e-5
	2	100		0.9502-1.0500		

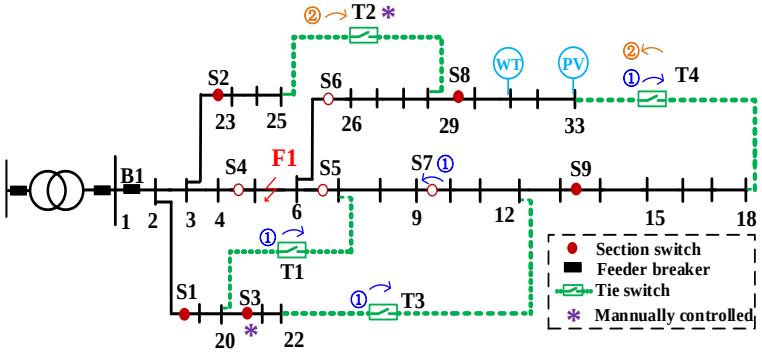

Fig. 4. Supply restoration configuration in Scheme I.

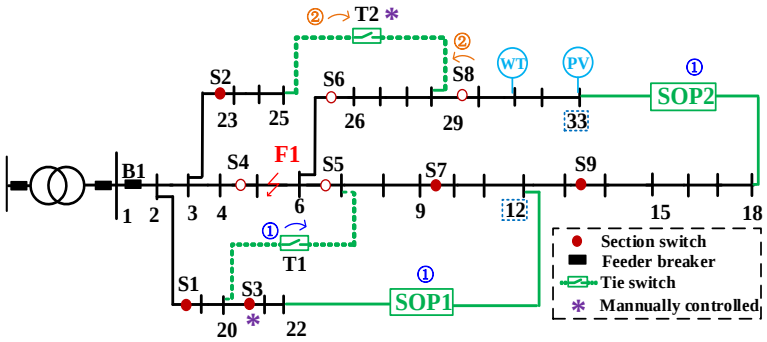

Fig.5. Supply restoration configuration in Scheme II.

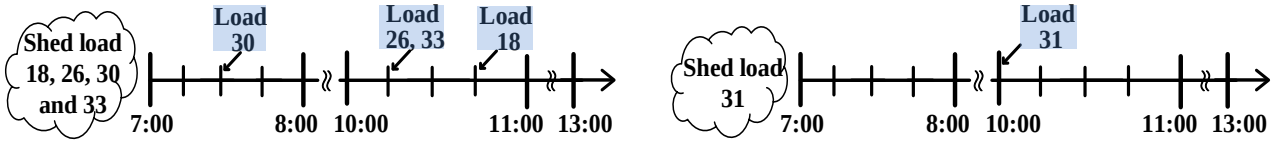

(a) Scheme I **(b) Scheme II**

Fig. 6. Load pick-up schedule in the supply restoration period.

For Scheme II with SOP integration, supply restoration is conducted with the multi-stage co-ordination of SOPs and switches in two stages. After fault isolation, SOP2 is de-energized while SOP1 remains energized. In the first stage, the control mode of SOP1 rapidly switches to provide voltage support for nodes 7 to 18. Then, as VSC at node 18 is energized, SOP2 can be activated to

provide voltage support to outage loads at nodes 26 to 33. To coordinate with the switching operation of T1, the control mode of SOP1 rapidly changes to PQ-U_{dc}Q control after T1 is closed. Thus, the critical loads can be rapidly picked up through the coordination of multiple SOPs and switching actions.

However, the restoration effect is limited by the capacity of SOPs. In the second stage, the relatively slow switching actions of T2 and S8 are coordinated with SOPs. The load recovery level is further improved even with increasing load consumption. The load pick-up schedule is shown in Fig. 6(b).

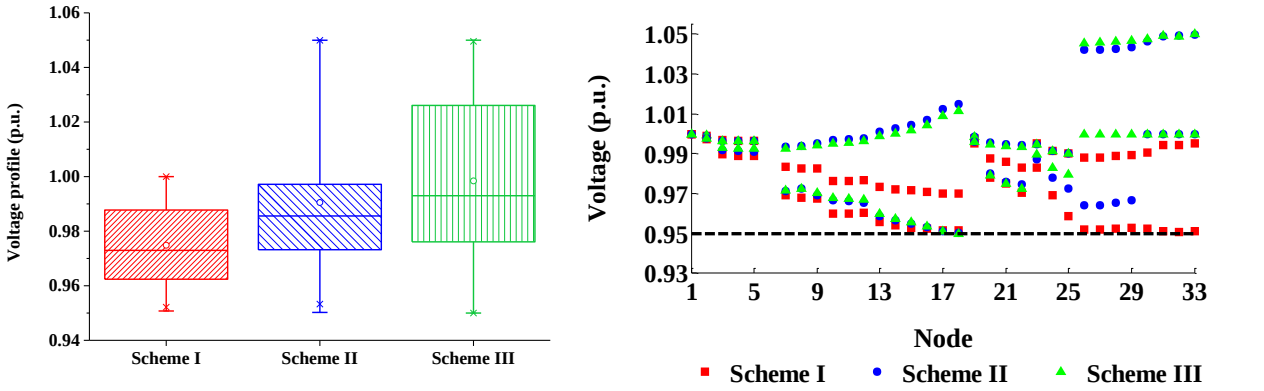

(a) Box plot of voltage profile **(b) Extreme value of node voltage**

Fig. 7. Voltage profiles in Schemes I, II and III.

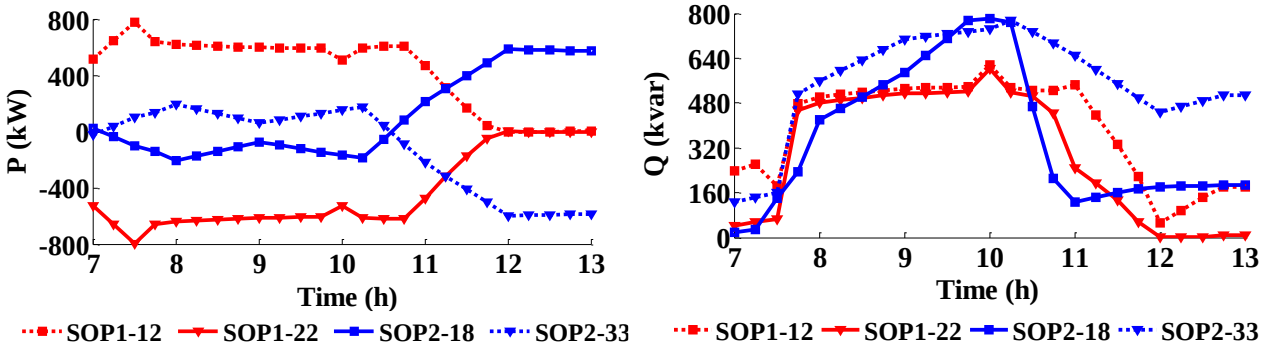

(a) Active power transmission of SOPs **(b) Reactive power outputs of SOPs**

Fig. 8. Supply restoration strategies of SOPs in Scheme II.

Fig. 7 depicts voltage profiles of Schemes I and II. As illustrated in Fig. 7, the average node voltage in Scheme I is lower than that in Scheme II, which severely restricts the load recovery

level. In Scheme II, voltage level is effectively improved through the voltage support provided by SOPs. Fig. 8 shows the supply restoration strategies of SOP1 and SOP2 in Scheme II. As shown in Fig. 8, SOP can also provide reactive power to ensure node voltage within secure operation range.

2) Comparison with static restoration

To compare with the static restoration method, Scheme III is added under fault F1. Scheme III adopts fixed switching operation and SOP control mode throughout the entire period, as proposed in [13].

Scheme III: Static supply restoration is conducted based on the coordination of SOPs and switches.

The restoration results in Scheme III are described in Fig. 9. The comparison of restoration performance in Schemes II and III is listed in Table 4.

The static supply restoration in Scheme III gives the fixed restoration operation during the entire restoration process without considering the multi-stage coordination of SOPs and switches. Compared with Scheme III, the sequential switching operation is further coordinated with SOPs in Scheme II. It can be seen that Scheme II performs better in the restored load ratio and the energy not supplied is only 39.69% of that in Scheme III. Besides, the secure operation can be ensured during the entire multi-stage restoration process in Scheme II.

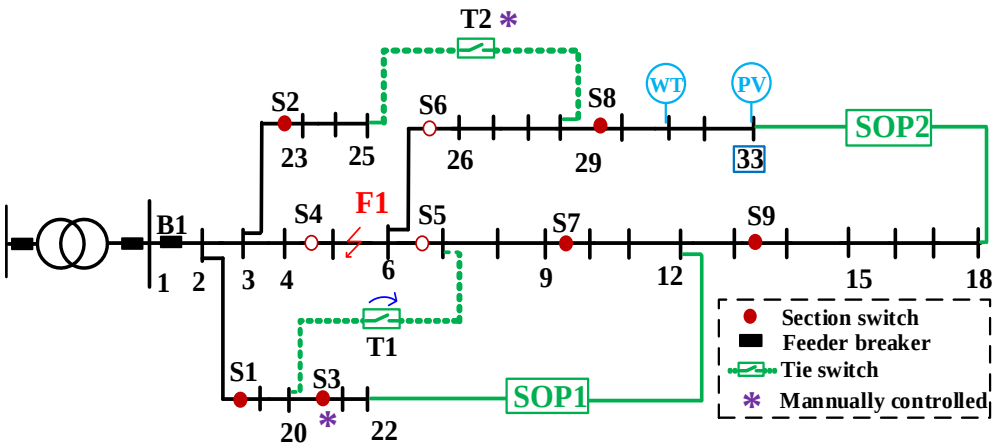

Fig.9. Supply restoration configuration in Scheme III.

Table 4 Performance comparison of Schemes II and III

Scheme	Restored ratio of active power of load (%)	Energy not supplied (kWh)	Voltage range (p.u.)	Computation time (s)
II	100	395.6250	0.9502-1.0500	138.41
III	89.97	921.2500	0.9500-1.0500	27.33

As shown in Table 4, the proposed multi-stage model is with a longer computation time than the static method due to the larger number of variables. Thus, online analysis based on the proposed method cannot meet the requirements of rapid supply restoration. The widely used contingency set can be used to implement the supply restoration strategy. As for the proposed restoration method, the contingency set can be established one day ahead including the multi-stage restoration strategies to all critical faults. In real-time operation, the specific restoration strategy matching the fault will be selected once the fault is located and isolated. The operation sequence of SOPs and switches can be deployed immediately, which effectively enhances the accuracy and effectiveness of restoration.

5.3. Practical distribution networks with four terminal SOP

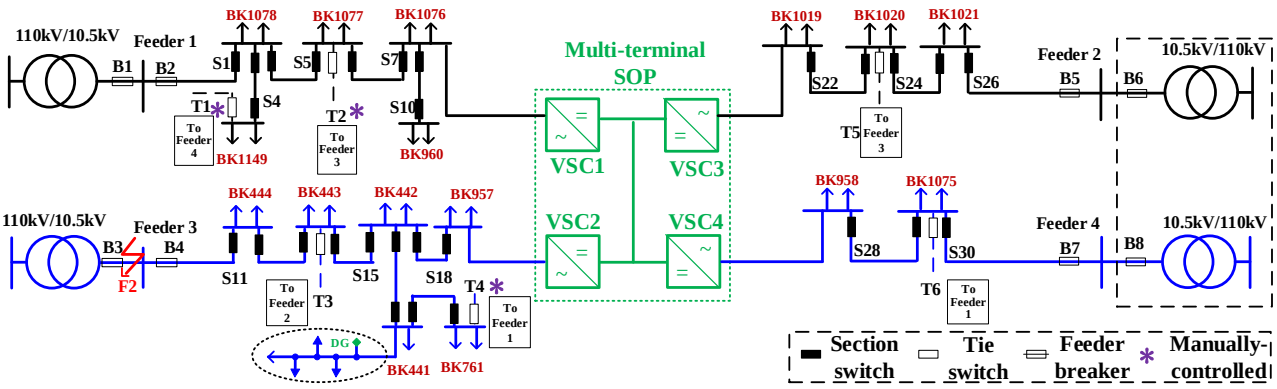

Fig. 10. Structure of the practical distribution networks in Tianjin.

Practical distribution networks with four-terminal SOP in Tianjin are adopted to further verify

the applicability of the proposed multi-stage method, as shown in Fig. 10. The practical case includes three substations, of which the rated voltage level is 10.5 kV. The parameters of DG are listed in Table 5. The capacity of each converter of multi-terminal SOP is set as 1.0 MVA. The desired voltage range is [0.95, 1.05] (p.u). It is assumed that a permanent three-phase fault occurs at the beginning of Feeder 3, defined as fault F2. The other parameters are set to the same values as the modified IEEE 33-node system.

Table 5 Installation capacities of DGs

Feeder	PV (MVA)	WT (MVA)
1	1.5	-
2	-	0.6
3	0.5	1.2
4	0.5	0.6

Under fault F2, switches B3 and B4 are operated initially to isolate the fault. After fault isolation, all the loads and DGs of Feeder 3 are out of service. The total outage active power reaches 2515.0 kW. Schemes I and II are respectively conducted for supply restoration.

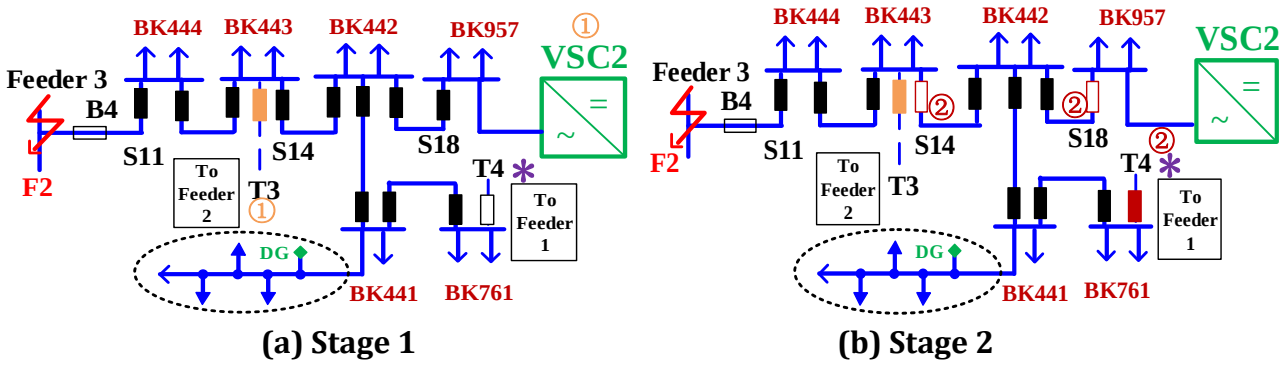

Fig. 11. Supply restoration stages in Scheme II under fault scenario F2.

Table 6 Restoration results of Schemes I and II

Scheme	Stage	Restored ratio of active power of load (%)	Energy not supplied (kWh)	Voltage range (p.u.)
I	1 (7:00-7:30)	92.45	311.4063	0.9500-1.0008

	2 (7:31-9:00)	96.02		0.9585-1.0000
	3 (9:01-13:00)	98.18		0.9508-1.0000
II	1 (7:00-7:30)	100	0.0000	0.9545-1.0000
	2 (7:31-13:00)	100		0.9502-1.0000

Table 6 shows the multi-stage supply restoration results of Schemes I and II. The conventional switch-based restoration in Scheme I requires three-stage coordination, while the proposed method in Scheme II requires two stages. Compared with conventional switches, The SOP integration in Scheme II facilitates the fast restoration of ADNs. Based on the sequential coordination of the multi-terminal SOP and switching actions, the restoration performance in Scheme II outperforms that in Scheme I within the secure voltage range.

The detailed restoration in Scheme II is depicted in Fig. 11. In the first stage, VSC2 of SOP changes to $U_{dc}Q$ control rapidly to provide voltage support to Feeder 3 before closing automated tie switch T3. Then, T3 provides voltage support and VSC2 turns to PQ control to provide power support. All the loads are picked up in the first stage. Then in the second stage, the relatively slow operation of T4 closing is coordinated with the $U_{dc}Q$ control of VSC2 and the opening of S14 and S18. Thus, VSC2, T3 and T4 provide voltage support to different parts of Feeder 3, respectively. The coordinated restoration operation in the second stage is aimed to further enhance the secure operation under the increased load level.

Similar to the analysis in Section 5.2, the load recovery level is effectively improved with secure operation of ADNs based on the multi-stage coordination of SOPs and switches in supply restoration

6. Conclusion

This paper proposes a multi-stage supply restoration method with SOPs for ADNs, in which the sequential switching actions are coordinated with flexible control modes of SOPs during the entire restorative process. First, the impact of SOP control mode on the supply restoration sequence is analyzed. By providing voltage support, the coordination of multiple SOPs will rapidly energize the outage area and improve the voltage profile. Then, a multi-stage supply restoration model with SOPs is proposed to maximize the load recovery level of ADNs. The coordinated switching actions and SOP control mode selection can be given in sequence, which is more practical for application. Besides, the secure operation is ensured during the entire restoration period through formulating the restoration sequence. Finally, the effectiveness of the proposed restoration method is validated on a modified IEEE 33-node distribution system and practical distribution networks with four-terminal SOP in Tianjin. Results show that the proposed method can fully exploit potential benefits of SOPs and effectively improve load recovery level of ADNs.

There are several interesting directions for our future work. Supply restoration should further consider the uncertainties of DG, which can be effectively solved by distributed robust optimization. This is expected to effectively cope with the DG fluctuation. As the restoration performance of SOP is limited by its capacity and location, the optimal siting and sizing problem of SOPs is worth investigation to maximize the restoration ability of SOPs.

Acknowledgments

This work was supported by the National Natural Science Foundation of China (51961135101, 52007131), National Postdoctoral Program for Innovative Talents (BX20190229), China Postdoctoral Science Foundation (2020M670652) and Swedish Research Council (2018-06007).

References

[1] Zhang S, Chang H, et al. Probabilistic evaluation of available load supply capability for distribution system. IEEE Trans Power Syst, 2013; 28(3): 3215-25..

[2] Sedighizadeh M, Esmaili M, Esmaeili M. Application of the hybrid Big Bang-Big Crunch algorithm to optimal reconfiguration and distributed generation power allocation in distribution systems. Energy 2014; 76: 920-30.

[3] Bloemink J M and Green T C. Benefits of distribution-level power electronics for supporting distributed generation growth. IEEE Trans Power Deliv 2013; 28(2): 911-9.

[4] Shen Y, Gu C, Ma Z, et al. A two-stage resilience enhancement for distribution systems under hurricane attacks. IEEE Syst J 2021; 15(1): 653-61.

[5] Cao W, Wu J, Jenkins N, et al. Benefits analysis of soft open points for electrical distribution network operation. Appl Energy 2016; 165: 36-47.

[6] Wang Z and Wang J. Self-healing resilient distribution systems based on sectionalization into microgrids. IEEE Trans Power Syst 2015; 30(6): 3139-49.

[7] Niu G, et al. A fast power service restoration method for distribution network with distributed generation. Proc. IEEE Trans. Electrific Conf Expo, Asia-Pacific 2017: 1–6.

[8] Liu W, Lin Y, Zhang S, et al. Research on Dynamic Reconfiguration of Distribution Network with High Penetration of DG. 2021 3rd Asia Energy and Electrical Engineering Symposium (AEEES) 2021: 433-7.

[9] Sekhavatmanesh H and Cherkaoui R. Analytical approach for active distribution network restoration including optimal voltage regulation. IEEE Trans Power Syst 2019; 34(3), 1716-28.

[10] Li W, Li Y, Chen C, et al. A full decentralized multi-agent service restoration for distribution network with DGs. IEEE Tran Smart Grid 2020; 11(2): 1100-11.

[11] Aithal A, Li G, Wu J, et al. Performance of an electrical distribution network with soft open point during a grid side AC fault. Appl Energy 2016; 227: 262-72.

[12] Picioroaga I, Tudose A, et al. Application of soft open points for increasing the supply restoration in active distribution networks. 2021 12th International Symposium on Advanced Topics in Electrical Engineering (ATEE), 2021: 1-6.

[13] Li P, Ji J, Ji H. Self-healing oriented supply restoration method based on the coordination of multiple SOPs in active distribution networks. Energy 2020; 195: 1-11.

[14] Wang J, Zhou N and Wang Q. Data-driven stochastic service restoration in unbalanced active distribution networks with multi-terminal soft open points. Int J Electr Power Energy Syst 2020; 121, 106069.

[15] Chen B, Chen C, Wang J, et al. Sequential service restoration for unbalanced distribution systems and microgrids. IEEE Trans on Power Syst 2018; 33(2): 1507-20.

[16] Tian S, Wang X, Wang X, et al. Network transition security for transmission switching. J Mod Power Syst Clean Energy 2019; 7(5): 1105-14.

[17] Wang P and Li W. Reliability evaluation of distribution systems considering optimal restoration sequence and variable restoration times. IET Energy Syst Integr 2007; 1(4): 688-95.

[18] Azizivahed A, Narimani H, Fathi M, et al. Multi-objective dynamic distribution feeder reconfiguration in automated distribution systems. Energy 2018; 147: 896-914.

[19] Li Y, Xiao J, Chen C, et al. Service restoration model with mixed-integer second-order cone programming for distribution network with distributed generations. IEEE Trans Smart Grid 2019; 10(4): 4138-50.

[20] Jabr R. A, Singh R and Pal B. C. Minimum loss network reconfiguration using mixed-integer convex programming. IEEE Trans Power Syst 2012; 27(2): 1106-15.

[21] Chen B, Ye Z, Chen C, et al. Toward a MILP modeling framework for distribution system restoration. IEEE Trans Power Syst 2019; 34(3): 1749-60

[22] Chen B, Ye Z, Chen C, et al,. Toward a synthetic model for distribution system restoration and crew dispatch. IEEE Trans Power Syst 2019; 34(3): 2228-39.

[23] Ding T, Wang Z, Jia W, et al. Multiperiod distribution system restoration with routing repair crews, mobile electric vehicles, and soft-open-point networked microgrids. IEEE Trans Smart Grid 2020; 11(6): 4795-808.

[24] Wang F, Chen C, Li C, et al. A Multi-stage restoration method for medium-voltage distribution system with DGs. IEEE Trans Smart Grid 2017; 8(6): 2627-36.

[25] Sekhavatmanesh H and Cherkaoui R. A multi-step reconfiguration model for active distribution network restoration integrating DG start-up sequences. IEEE Trans Sust Energy 2020; 11(4): 2879-88.

[26] Wang Y, Xu Y, Li J, et al. On the radiality constraints for distribution system restoration and reconfiguration problems. IEEE Trans Power Syst 2020; 35(4): 3294-6.

[27] Lavorato M, Franco J. F, Rider M. J and Romero R. Imposing radiality constraints in distribution system optimization problems. IEEE Trans Power Syst; 27(1): 172-80.

[28] Huang X, Yang Y and Taylor A. G. Service restoration of distribution systems under distributed generation scenarios. CSEE J Power Energy Syst 2016; 2(3): 43-50.

[29] Baran M. E, Mesut and Wu F. Optimal sizing of capacitors placed on a radial distribution system. IEEE Trans Power Deliv 1989; 4(1): 725-34.

[30] Zhang S, Cheng H, et al. Distributed generation planning in active distribution network considering demand side management and network reconfiguration. Appl Energy 2018; 228: 1921-36.

[31] Li P, Ji J, Wang C, et al. Coordinated control method of voltage and reactive power for active distribution networks based on soft open point. IEEE Trans Sust Energy 2017; 8(4): 1430-42.

[32] Li P, Ji J, Ji H, et al. MPC-based local voltage control strategy of DGs in active distribution networks. IEEE Trans Sust Energy 2020; 11(4): 2911-21.

[33] Lavaei J and Low S H. Zero duality gap in optimal power flow problem. IEEE Trans Power Syst 2012; 27(1): 92-107.

[34] Low S H. Convex relaxation of optimal power flow, I: Formulations and relaxations. IEEE Trans Control Netw Syst 2014; 1(1): 15-27.

[35] Lofberg J. Yalmip: A toolbox for modeling and optimization in MATLAB. IEEE International Symposium on Computer Aided Control Systems Design 2004; 284-9.

[36] Baran M, Wu F. Optimal capacitor placement on radial distribution systems. IEEE Trans Power Deliv 1989; 4(1): 725-34.